Proceedings of the 21st ICSMGE, Vienna, Austria, 14 – 19 June 2026. Pistrol, Adam & Schweiger (eds.)
Published by: ÖGG, Austrian Society for Geomechanics, Salzburg, Austria, ISBN 978-3-9503898-4-5
https://doi.org/10.53243/ICSMGE2026-1637

The effect of groundwater table on the bearing capacity of shallow foundations: An earth pressure analysis approach

Lysandros Pantelidis
Cyprus University of Technology Cyprus, lysandros.pantelidis@cut.ac.cy

Eleyas Assefa
Addis Ababa Science and Technology University, Ethiopia

Costas Sachpazis
University of Western Macedonia, Greece

ABSTRACT: This paper presents a new analytical method for assessing the bearing capacity of shallow foundations under the influence of groundwater table fluctuations. Unlike existing empirical approaches, which often rely on semi-graphical interpretations or introduce water table factors through separate assumptions, the proposed method derives groundwater correction factors directly from the same classical earth pressure-based analysis previously used for the derivation of the bearing capacity N-factors. This consistency ensures a unified and rigorous theoretical framework. The groundwater table factors account for both cases of water level lying below and above the foundation base, providing simple, adaptable expressions for engineering practice. A detailed comparison with traditional methods (e.g., Meyerhof, Vesic, Hansen, AASHTO) reveals significant differences, highlighting the limitations of earlier approaches. Validation against finite element analyses performed with RS2 software shows excellent agreement, demonstrating the accuracy and robustness of the proposed method. The results confirm that the fully analytical procedure developed herein offers a reliable and comprehensive tool for predicting the bearing capacity of shallow foundations in the presence of groundwater.

KEYWORDS: Groundwater Table, Bearing Capacity, Shallow Foundations, Earth Pressure Analysis, Groundwater Table Factors

1 INTRODUCTION

The first study examining how submergence in sand affects its bearing capacity was conducted by Terzaghi in 1925. Terzaghi (1925) showed that when a footing is placed on fully submerged sand beneath a static water-table, the bearing capacity can be determined by the following equation:

$$q_u = \left[\tfrac{1}{2}\gamma' B N_\gamma\right]_{\text{Terzaghi}} = \tfrac{1}{2}\gamma B N_\gamma w_\gamma = \tfrac{1}{2}\gamma B N_\gamma \left[\frac{\gamma'}{\gamma}\right]_{w_\gamma} \quad (1)$$

B is the width of the footing, γ and γ' are the bulk and submerged unit weights of soil, respectively, N_γ is the bearing capacity factor associated with the unit weight term, and $w_\gamma = \gamma'/\gamma$ is the corresponding groundwater table correction factor.

In the more general case where the groundwater table lies at a depth d_w below the foundation surface (not exceeding the depth of the theoretical failure zone), and the footing is embedded at a depth D_f (as shown in Figure 1a), the bearing capacity of strip footings, according to Meyerhof (1955), is:

$$q_u = \tfrac{1}{2}\gamma B N_\gamma \left[\frac{\gamma'}{\gamma} + F\left(1 - \frac{\gamma'}{\gamma}\right)\right]_{w_\gamma} + \gamma D_f N_q \text{ for } D_f \le B \quad (2)$$

F is a factor that ranges from 0 for fully submerged soils to 1 when the water table is at or below the depth of the theoretical failure zone.

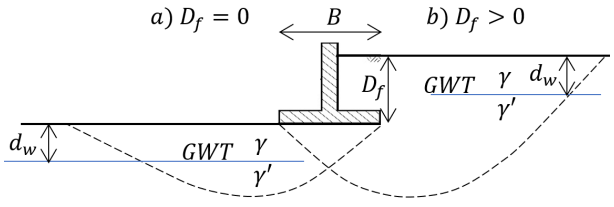

Figure 1. Bearing capacity problem showing groundwater table (GWT) at a depth a) below and b) above the foundation surface.

Meyerhof presented F values in chart form rather than as a formula. His approach involved summing two components. To derive the first component, he considered the soil as fully submerged (γ'), applying Equation 1 to calculate the bearing capacity. For the second component, Meyerhof employed a semi-graphical method that accounted for the difference in unit weight ($\gamma - \gamma'$) above and below the water table, with γ representing the unit weight between ground level and the water table, and γ' below it. Meyerhof provided $F - \varphi$ relationships for ratios of d_w/B at 0.1, 0.2, 0.3, 0.5, 1.0, 1.5, and 2.0, covering a range of $14.7° \le \varphi \le 50°$. According to his findings, the bearing capacity is affected by the water table if it is located between the foundation base and a depth of approximately twice the foundation width.

For the case where the water table is located between the ground surface and the foundation base, Meyerhof suggested the following:

$$q_u = \tfrac{1}{2}\gamma B N_\gamma \left[\frac{\gamma'}{\gamma}\right]_{w_\gamma} + \gamma D_f N_q \left[\frac{\gamma'}{\gamma} + \left(1 - \frac{\gamma'}{\gamma}\right)\frac{d_w}{D_f}\right]_{w_q} \quad (3)$$

d_w is measured from the ground surface (i.e., $0 \le d_w \le D_f$).

Vesic (1973, 1975) suggested a linear increase of w_γ with d_w, and consequently of q_u:

$$q_u = \tfrac{1}{2}\gamma B N_\gamma \left[\frac{\gamma'}{\gamma} + \frac{d_w}{B}\left(1 - \frac{\gamma'}{\gamma}\right)\right]_{w_\gamma} + \gamma D_f N_q \quad (4)$$

According to Vesic, the water table has no influence on the bearing capacity if $d_w > B$.

Equations 3 and 4 are widely used in practice, although the following variation for w_γ and w_q can also be found (e.g., IS6403 (1981), AASHTO (2020), FHWA (Kimmerling, 2002)):

$$w_\gamma = 0.5 + 0.5\frac{d_w}{D_f + 1.5B} \le 1.0 \quad (5)$$

$$w_q = 0.5 + 0.5\frac{d_w}{D_f} \le 1.0 \quad (6)$$

In both Equations 5 and 6 d_w is measured from the ground surface (and not from the foundation surface).

Upon comparing Equation 6 with the corresponding w_q term in Equation 3, it becomes evident that the ratio γ'/γ has been replaced by a fixed value of 0.5. The same applies to Equation 5, while in the w_γ expression in question, $F =$

$d_w/(D_f + 1.5B)$. In this factor, the depth of the failure zone, H_{max}, is assumed to be equal to $1.5B$ regardless of the soil's friction angle. However, it is well known that this depth depends on the friction angle of the soil, and it is generally accepted that for $D_f = 0$ it is given by Equation 7, derived from the log-spiral equation $r = r_o e^{a\tan\varphi}$ (Zone II), which connects the two linear parts of Zones I and III (Figure 2)

$$H_{max} = \frac{B}{2}\frac{\cos\varphi}{\cos\left(\frac{\pi}{4}+\frac{\varphi}{2}\right)} e^{\left(\frac{\pi}{2}+\frac{\varphi}{2}\right)\tan\varphi} \quad (7)$$

The axis of rotation of the log spiral aligns with the edge of the footing on the anticipated failure side. The radius r_o corresponds to the length of the side of the triangular elastic zone beneath the foundation (Zone I), forming an angle of $45^o + \varphi/2$ with the horizontal foundation surface. The failure surface emerges at an angle of $45^o - \varphi/2$ with the horizontal surface at the foundation level. This configuration has been experimentally validated, among others, by Vesic (1975) as approximately correct.

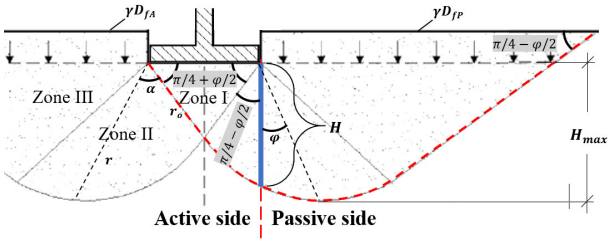

Figure 2. Geometric characteristics of the bearing capacity failure problem.

Krishnamurthy and Rao (1975) explored the impact of soil submergence on the bearing capacity of strip foundations using the method of characteristics. They offered modified values for the bearing capacity factor N_γ at γ/γ' ratios of 0.48, 0.57, and 0.7, with φ varying from 15° to 40° in 5° increments. According to their findings, the water table has no influence on the bearing capacity if $d_w > 1.2B$.

Simone and Zurlo (1987) also used the method of characteristics to suggest w_γ values in chart form for smooth and rough footings for $\varphi = 30^o$ and 45°.

Hansen et al. (1987) derived the following bearing capacity equation for footings on cohesionless soils without lateral surcharge:

$$q_u = \frac{1}{2}\gamma B N_\gamma \left[\frac{\gamma'}{\gamma} + \frac{d_w}{H_{max}}\left(2 - \frac{d_w}{H_{max}}\right)\left(1 - \frac{\gamma'}{\gamma}\right)\right]_{w_\gamma} + c_f N_c \left[\frac{d_w}{H_{max}}\right]_{w_c} + \gamma_w h_c (N_q - 1)\left(1 - \frac{d_w}{H_{max}}\right) \quad (8)$$

with $N_q = e^{\pi\tan\varphi}(1 - \sin\varphi)/(1 + \sin\varphi)$. The second term is related to the apparent cohesion of the moist sand above the water table, while the third term accounts for the weight of water trapped in the capillary zone (h_c is the height of this zone). Referring to their calculations, Hansen et al. noted that for a wide range of values of φ the depth of the failure zone, H_{max}, is almost constant and equal to:

$$H_{max} = 1.125B\sin\left(\frac{\pi}{4}+\frac{\varphi}{2}\right) e^{\left(\frac{\pi}{4}+\frac{\varphi}{2}\right)\tan\varphi} \quad (9)$$

According to Bowles (1996), on the other hand:

$$w_\gamma = \frac{\gamma'}{\gamma} + \frac{d_w}{z_I}\left(2 - \frac{z_w}{z_I}\right)\left(1 - \frac{\gamma'}{\gamma}\right) \quad (10)$$

That is, it appears that Bowles replaced the H_{max} term in Hansen et al.'s formula with the height of the soil triangle defining Zone I, z_I. Geometrically, the latter is:

$$z_I = \frac{B}{2}\tan\left(\frac{\pi}{4}+\frac{\varphi}{2}\right) \quad (11)$$

Ausilio and Conte (2005) used the kinematic approach of limit analysis to propose analytical expressions for the upper bound bearing capacity of strip footings resting on a soil with the water table located at some depth below the footing base. They provided adjusted N_γ^* factors, from which the w_γ factor can be derived:

$$w_\gamma = \frac{N_\gamma^*}{N_\gamma} = \frac{\gamma'}{\gamma} + \frac{d_w}{B}\left(1 - \frac{\gamma'}{\gamma}\right)\frac{N_{\gamma w}}{N_\gamma} \quad (12)$$

Ausilio and Conte developed expressions for N_γ and $N_{\gamma w}$, with the latter derived for three distinct scenarios: $0 \le d_w \le z_I$, $z_I \le d_w \le z_{II}$ and $z_{II} \le d_w < H_{max}$, where, z_I and z_{II} represent the lowest points of Zones I and II, respectively, in Prandtl's (1920) mechanism, while H_{max} denotes the depth of the failure zone, as defined by the following expression:

$$H_{max} = B\frac{\cos\varphi}{2\cos\left(\frac{\pi}{12}+\varphi\right)} e^{\frac{5}{12}\pi\tan\varphi} \quad (13)$$

The expressions for N_γ and $N_{\gamma w}$ proposed by Ausilio and Conte are overly complex for manual calculations.

Utilizing the method of characteristics, Cascone et al. (2021) proposed that:

$$w_\gamma = \frac{\gamma'}{\gamma} + \frac{\gamma_w}{\gamma}\frac{d_w}{H_{max}}\left(2.626\left(1 - \frac{d_w}{H_{max}}\right) + \left(\frac{d_w}{H_{max}}\right)^2\right) \quad (14)$$

For Cascone et al. the depth of the failure zone, H_{max}, for smooth and rough footings is:

$$H_{max} = \begin{cases} \left(0.146\frac{1+\sin\varphi}{1-\sin\varphi} - 0.047\right)B \text{ (smooth)} \\ \left(0.299\frac{1+\sin\varphi}{1-\sin\varphi} - 0.132\right)B \text{ (rough)} \end{cases} \quad (15)$$

In the following section, the various formulas related to the depth of the failure zone are discussed. Subsequently, new expressions for the w_γ and w_q factors will be proposed. These factors will be derived by treating the problem as a classical earth pressure analysis problem. It is important to be noted that since groundwater affects the unit weight of soil, w_c is consistently equal to unity ($w_c = 1$).

2 DEPTH OF THE FAILURE ZONE

There is no doubt that the depth of failure should exceed the depth where Zone I extends below the footing (i.e., $H_{max} > z_I$). For vertically applied loading, it is commonly assumed that Zone I has the shape of an equilateral triangle, with the two angles in contact with the footing equal to $45° + \varphi/2$. This is a rational assumption based on the orientation of principal stresses within the soil. More specifically, under a vertical loading, the maximum principal stress is vertical, while the minimum principal stress is horizontal. In such a scenario, the planes of maximum shear stress are oriented at 45° to the principal stress directions. The addition of the soil's internal friction angle, φ, further influences the failure mechanism. The soil's resistance to shear along these planes is a function of both the normal stress and the internal friction, as described by the Mohr-Coulomb failure criterion. Consequently, the failure plane is inclined at an angle of $45° + \varphi/2$ from the horizontal. Furthermore, based on finite element and regression analysis, Pantelidis (2023) found that H_{max} given by Equation 7 requires a correction factor. More specifically, the corrected H_{max} for rigid footings is:

$$H_{max} = \kappa\left(1 + 0.2\frac{D_f}{B}\right)\frac{B}{2}\frac{\cos\varphi}{\cos\left(\frac{\pi}{4}+\frac{\varphi}{2}\right)} e^{\left(\frac{\pi}{4}+\frac{\varphi}{2}\right)\tan\varphi},$$

$$\kappa = \begin{cases} 0.993 \approx 1, & \psi = 0° \\ 1.115 \approx 1.12, & \psi = \varphi \end{cases} \quad (16)$$

The term $\kappa(1+0.2D_f/B)$ is the depth factor in the bearing capacity equation recently proposed by Pantelidis (2023). From Equations 7, 9, 13, 15 and 16, it is clear that for $D_f = 0$, the H_{max}/B ratio depends only on φ. The corresponding H_{max}/B versus φ relationships are plotted in Figure 3 for comparison. Several important observations can be made from the figure. First, the $\kappa = 0.993 \approx 1$ value for $\psi = 0°$ strongly suggests that Prandtl's failure mechanism with three zones is an excellent approximation for soils obeying the non-associated flow rule. On the other hand, the value $\kappa = 1.115 \approx 1.12$ value indicates that the soils with $\psi = \varphi$ require a failure mechanism approximately 12% dipper. This value directly compares to Hansen et al.'s (1987) factor of 0.125. It should be noted that Hansen et al.'s formula pertains to soils following the associated flow rule with $\psi = \varphi$. Hansen et al.'s H_{max} can be rewritten as follows, with the similarity with the proposed formula in Equation 16 more than evident:

$$H_{max,\text{Hansen}} = 1.125B\sin\left(\frac{\pi}{4}+\frac{\varphi}{2}\right)e^{\left(\frac{\pi}{4}+\frac{\varphi}{2}\right)\tan\varphi} = \left[1.125\left[\frac{B}{2}\frac{\cos\varphi}{\cos\left(\frac{\pi}{4}+\frac{\varphi}{2}\right)}e^{\left(\frac{\pi}{4}+\frac{\varphi}{2}\right)\tan\varphi}\right]_{\psi=0}^{\text{Eq.7}}\right]_{\psi=\varphi} \quad (17)$$

Ausilio and Conte's limit analysis formula for H_{max} (Equation 13), on the other hand, produces a $H_{max}/B-\varphi$ curve that lies below the corresponding curve drawn using Equation 7 (and also Equation 16 for $\psi = 0$) is almost parallel to it. For direct comparison, Equation 13 can be rewritten as $H_{max,Eq.13} = (0.73 + 0.14\tan^{0.8}\varphi)H_{max,Eq.7}$ where the term in brackets ranges between 0.73 and 0.87 for $\varphi = 0$ and 45 degrees respectively. The authors have shown above that H_{max} from Equation 7 and $1.12H_{max,Eq.7}$ are good approximations of the actual maximum depth of the failure surface for $\psi = 0$ and $\psi = \varphi$, respectively. Ausilio and Conte's formula, however, returns small values for H_{max}; indeed, for $\varphi = 0$ H_{max} is approximately equal to z_I, which rather corresponds to a not acceptable failure mechanism. The same issue applies to the formulas by Cascone et al. for H_{max} for smooth and rough footings (Equation 15), which yield H_{max} values even smaller than z_I.

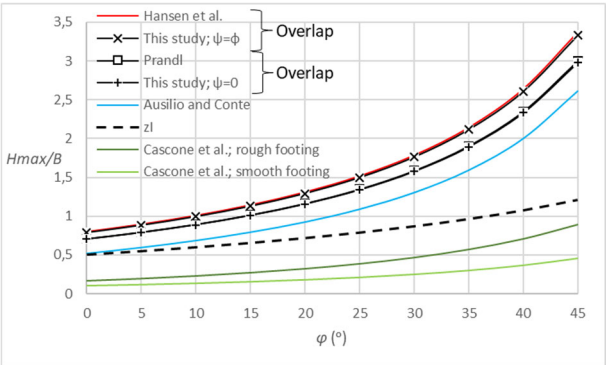

Figure 3. H_{max}/B versus φ comparison chart.

3 THE SUGGESTED GROUND-WATER TABLE FACTORS

A strip footing is assumed to be founded at depth D_f, although the foundation depth could vary on the two sides of the footing. Prandl's (1920) failure surface is generally adopted. However, the soil mass bounded by this surface, on the side of the footing where failure is expected to occur, is divided into an active failure zone beneath the footing and a passive failure zone extending beyond the edge of the footing (refer to Figure 2). These two zones are separated by a smooth, vertical, virtual wall of height H:

$$H = \kappa\left(1+0.2\frac{D_f}{B}\right)\frac{B}{2}\frac{e^{\left(\frac{\pi}{4}-\frac{\varphi}{2}\right)\tan\varphi}}{\cos\left(\frac{\pi}{4}+\frac{\varphi}{2}\right)} \quad (18)$$

Two cases are distinguished. In the first case the groundwater table lies at depth d_w below the foundation level, while in the second case the groundwater table is above the foundation level.

3.1 *Groundwater table below the foundation level*

In this case d_w is measured from the foundation level. Assuming that the soil is homogeneous and isotropic, and is subjected only to its own weight and the load from a uniformly loaded strip footing (which includes the self-weight of the footing), the following equation represents the balance of forces on both sides of the virtual wall at the time of the ultimate footing load, q_u:

$$\left[\int_0^H K_A(q_u-\gamma D_{f,A})I_z dz\right]_{A1} + \left[\int_0^H K_A(\gamma D_{f,A})dz\right]_{A3} + \left[\int_{d_w}^H \gamma_w(z-d_w)dz\right]_W +$$

$$+\left[\int_0^{d_w} K_A\gamma z dz + \int_{d_w}^H K_A\left(\gamma d_w+\gamma'(z-d_w)\right)dz - \int_0^H 2c\sqrt{K_A}dz\right]_{A2} =$$

$$= \left[\int_0^H 2c\sqrt{K_P}dz + \int_0^{d_w} K_P\gamma z dz + \int_{d_w}^H K_P\left(\gamma d_w+\gamma'(z-d_w)\right)dz\right]_{P1} +$$

$$\left[\int_0^H K_P(\gamma D_{f,P})dz\right]_{P2} + \left[\int_{d_w}^H \gamma_w(z-d_w)dz\right]_W \quad (19)$$

I_z is an influence factor that converts the vertical load at the foundation level into a horizonal load along the height of the virtual retaining wall (it is discussed further below). Elements $[A2]$ and $[P1]$ in Equation 19 refer to the earth pressures on the active and the passive sides of the virtual wall, respectively (see Figure 4). Elements $[A3]$ and $[P2]$ represent the lateral pressures on the wall caused by the lateral surcharges. For simplicity, the $\gamma D_{f,A}$ surcharge also assumed to start from the location of the virtual wall. However, for avoiding duplication, this surcharge is subtracted by q_u, as shown in the element $[A1]$.

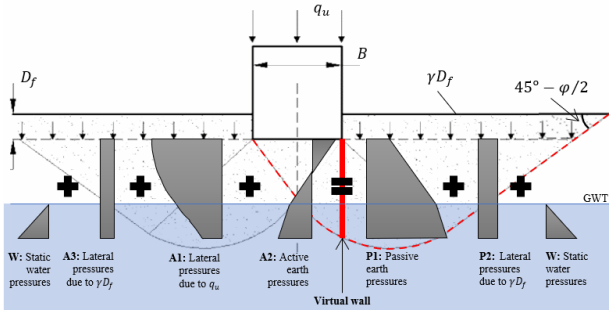

Figure 4. Forces acting on the virtual wall separating the active and passive zones when the groundwater table is below the foundation level (not to scale).

Solving Equation 19 for q_u and after rearranging the terms so that the resulting expression follows the basic bearing capacity equation structure with three terms, q_u is given by:

$$q_u = cN_c w_c + \frac{1}{2}\gamma B N_\gamma w_\gamma + \gamma D_{fP} N_q w_q \quad (20)$$

with

$$w_c = 1 \quad (21)$$

$$w_\gamma = \begin{cases} \frac{\gamma'}{\gamma} + \left(2 - \frac{d_w}{H}\right)\left(1 - \frac{\gamma'}{\gamma}\right)\frac{d_w}{H} \text{ for } 0 \le d_w \le H \\ 1 \text{ for } d_w > H \end{cases} \quad (22)$$

$$w_q = 1 \quad (23)$$

and

$$N_c = 2\frac{\sqrt{K_P}+\sqrt{K_A}}{K_A}\frac{H}{\int_0^H I(z)dz} \quad (24)$$

$$N_\gamma = \frac{K_P - K_A}{K_A}\frac{H}{B}\frac{H}{\int_0^H I(z)dz} \quad (25)$$

$$N_q = \frac{D_{f,A}}{D_{fP}} + \left(\frac{K_P}{K_A} - \frac{D_{f,A}}{D_{fP}}\right)\frac{H}{\int_0^H I_z dz} \quad (26)$$

The three $N-$factors were the subject of a previous study—see Pantelidis (2023)—and thus are not discussed herein. The static water pressures on the two sides of the virtual wall cancel each other out. The integral $\int_0^H I(z)dz$ represents the total horizontal force exerted on the wall by the footing, and its calculation is based on Boussinesq's theory. Since evaluating the integral requires the use of mathematical software, the authors, for convenience, provided the following best-fit expressions for both flexible and rigid footings:

$$\int_0^H I(z)dz = \begin{cases} -0.39\sin^3\varphi + 0.77\sin^2\varphi - 0.18\sin\varphi + 0.6 \text{ (rigid)} \\ 0.6\sin^2\varphi + 0.27\sin\varphi + 0.347 \text{ (flexible)} \end{cases} \quad (27)$$

3.2 *Groundwater table above the foundation level*

Here, d_w is measured from the ground surface on the passive side of the problem; it holds that $D_{fP} \le D_{fA}$. As before, the following equation represents the balance of forces on both sides of the virtual wall at the time of the ultimate footing load, q_u:

$$\left[\int_0^H K_A\left(q_u - \gamma(D_{fA} - D_{fP}) - \gamma d_w - \gamma'(D_{fP} - d_w)\right)I_z dz\right]_{A1} + \left[\int_0^H \gamma_w z dz\right]_W + \left[K_A\int_0^H \gamma' z dz - \int_0^H 2c\sqrt{K_A}dz\right]_{A2} + \left[\int_0^H K_A\left(\gamma(D_{fA} - D_{fP}) + \gamma d_w + \gamma'(D_{fP} - d_w)\right)dz\right]_{A3} = \left[\int_0^H 2c\sqrt{K_P}dz + \int_0^H K_P\gamma' z dz\right]_{P1} + \left[\int_0^H K_P\left(\gamma d_w + \gamma'(D_{fP} - d_w)\right)dz\right]_{P2} + \left[\int_0^H \gamma_w z dz\right]_W \quad (28)$$

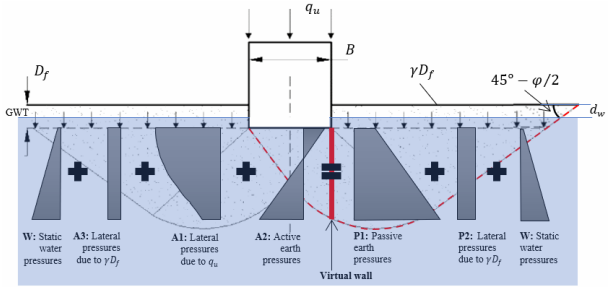

Figure 5. Forces acting on the virtual wall when the groundwater table is above the foundation level (not to scale).

Solving Equation 26 for q_u and expressing the solution in the same form as Equation 19, the following groundwater factors were obtained, while the $N-$factors remained unchanged (refer to Equations 23-25):

$$w_c = 1 \quad (29)$$

$$w_\gamma = \frac{\gamma'}{\gamma} \quad (30)$$

$$w_q = \frac{\left(\left(\frac{d_w}{D_{f,P}}\left(1-\frac{\gamma'}{\gamma}\right)+\frac{\gamma'}{\gamma}\right)\left(\frac{K_P}{K_A}-1\right)-\left(\frac{D_{f,A}}{D_{f,P}}-1\right)\right)\frac{H}{\int_0^H I(z)dz}+\left(\frac{D_{f,A}}{D_{f,P}}+\left(\frac{\gamma'}{\gamma}-1\right)\left(1-\frac{d_w}{D_{f,P}}\right)\right)}{N_q}$$

for $0 \le d_w \le D_{fP}$ (31)

For the special case of $D_{fP} = D_{fA} = D_f$, Equation 31 simplifies to Equation 32. In other words, the earth pressure analysis carried out by the authors reproduces Meyerhof's factors as presented in Equation 3.

$$w_q = \frac{\gamma'}{\gamma} + \left(1 - \frac{\gamma'}{\gamma}\right)\frac{d_w}{D_f} \text{ for } 0 \le d_w \le D_f \quad (32)$$

If the water table is above the foundation level, water may cause buoyancy problems to the foundation. This effect is beyond the scope of the present paper. The side resistance of foundations is also not considered here. Both issues are treated using conventional methods.

4 COMPARISON WITH EXISTING METHODS

The proposed w_γ factor of Equation 22 is compared with the corresponding factors proposed by Meyerhof, Vesic, Hansen, AASHTO and Bowles, given in Equations 2, 4, 8, 5 and 10, respectively. The results are presented in chart form in Figures 6a to 6e. These charts reveal generally great differences.

The same applies to the comparison against the w_γ factors proposed by Ausilio and Conte (2005) and Krishnamurthy and Rao (1975), as shown in Figures 7 and 8 respectively.

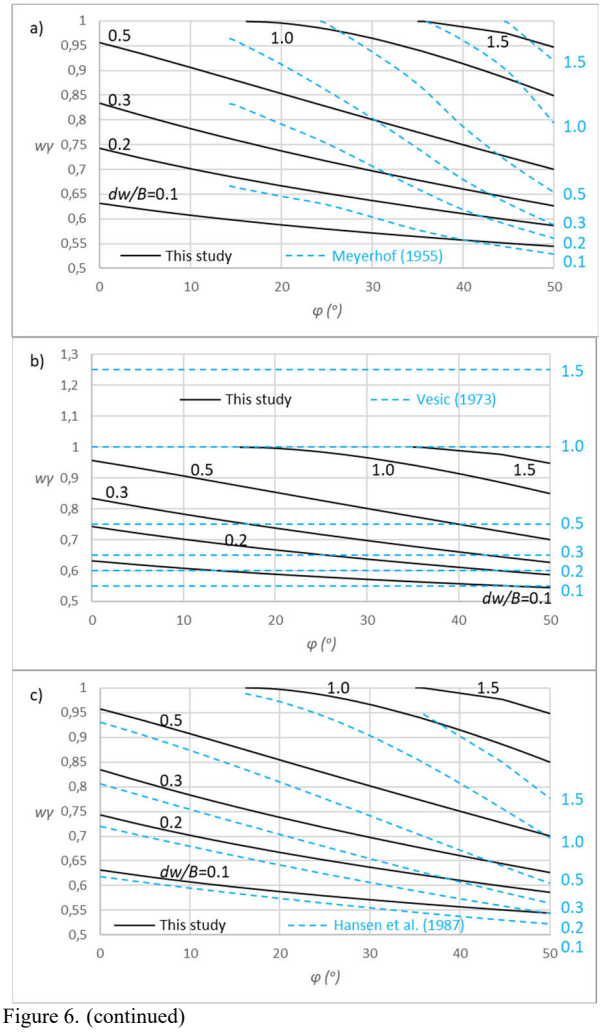

Figure 6. (continued)

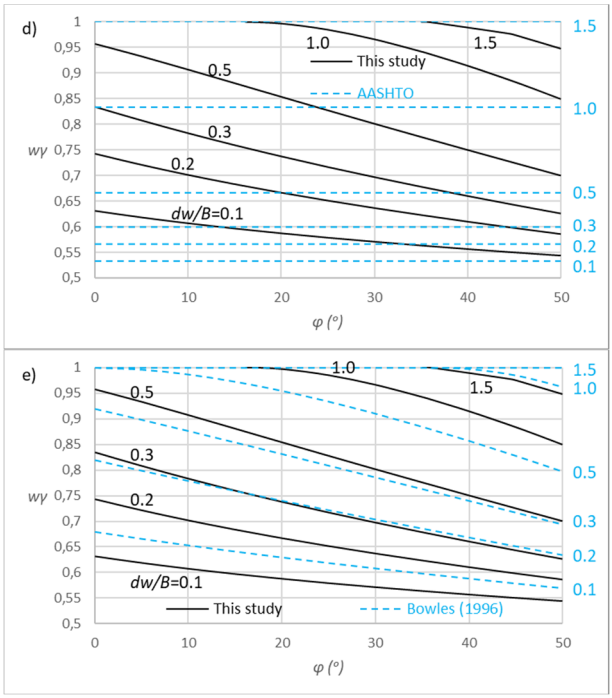

Figure 6. Charts comparing the proposed w_γ factor (Equation 22) with the respective factor proposed by a) Meyerhof, b) Vesic, c) Hansen, d) AASHTO and e) Bowles (Equations 2, 4, 8, 5 and 10 respectively)

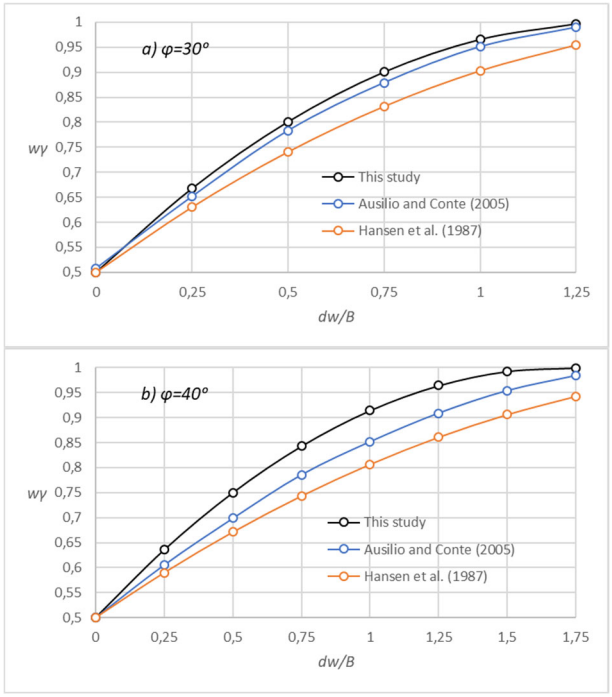

Figure 7. Chart comparing the w_γ factor of Ausilio and Conte (2005) and Hansen et al. (1987) and Rao (1975) with the proposed one for d_w/B ranging from 0 to 1.75. a) $\varphi = 30°$ and b) $\varphi = 40°$.1

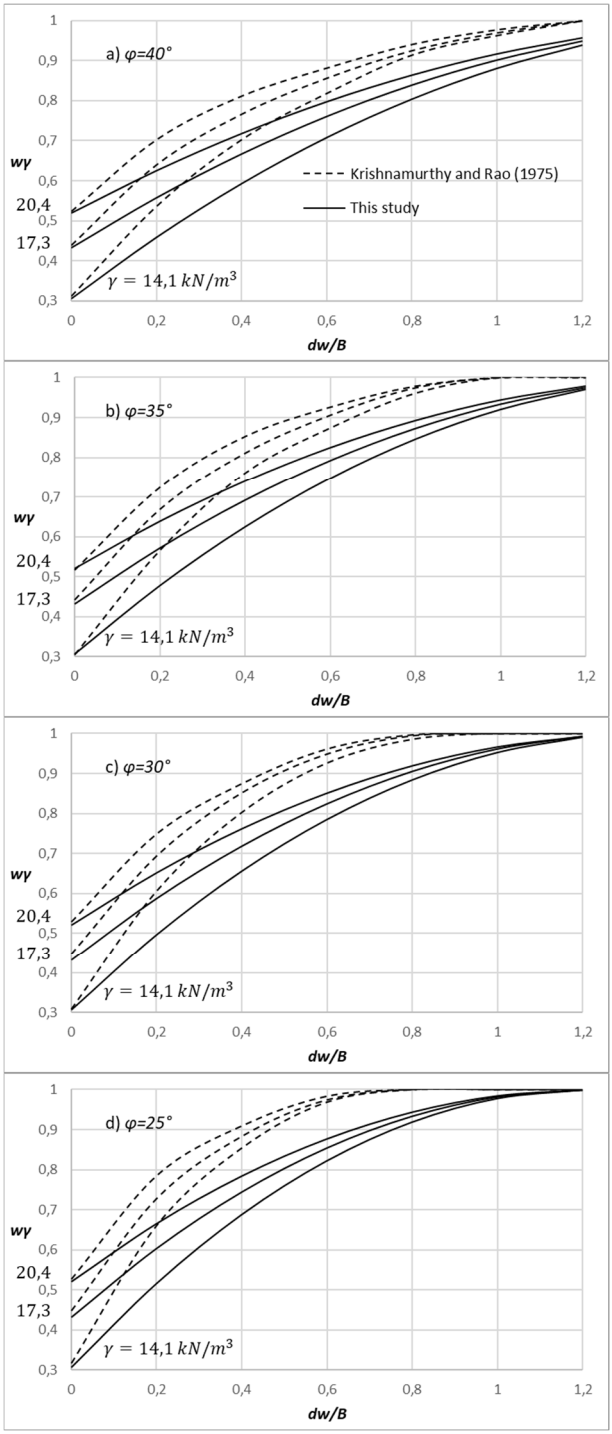

Figure 8. Charts comparing the w_γ factor of Krishnamurthy and Rao (1975) with the proposed one for φ =40, 35, 30 and 20° (a to d). Each chart includes three pairs of curves corresponding to γ =20.4, 17.3 and 14.1 kN/m^3.

5 APPLICATION EXAMPLE

A representative example is provided to demonstrate the applicability of the proposed analytical method. The finite element model, including its boundary conditions, geometry, and mesh, is shown in Figure 9. The model parameters were: rigid footing with width $B = 1.0\,m$, $D_f = 0\,m$, $c = 20\,kPa$, $\phi = 30°, \gamma = 17\,kN/m^3$, unit weight of water $\gamma_w = 9.81\,kN/m^3$, dilation angle $\psi = \varphi°$ and coefficient of earth pressure at rest $K_o = 0.5$. The analysis was performed for various positions

of the groundwater table, with the ratio d_w/B ranging from 0 to 2. Any data not explicitly shown in Figure 9 or not mentioned above can be found in Pantelidis (2023). The comparison results with the finite element method (FEM), performed using Rocscience's RS2 (v11.012) software, are presented in Figure 10. As can be observed, the results of the proposed analytical method exhibit excellent agreement with those of the FEM. For reference, the bearing capacity estimated by the AASHTO method is also included. The AASHTO results follow the same trend, although for this particular example they yield slightly lower values. Focusing on the groundwater table factors and favoring an objective comparison, the AASHTO factors $w_c = 1$ and $w_\gamma = 0.5 + 0.333 d_w/B$ were used along with Pantelidis' (2023) N-factors. The error introduced by the groundwater table factors alone ranges, for this specific example, from 8% to 13%. This is a considerable percentage, especially when one considers the errors associated with other factors, such as load eccentricity and inclination (Pantelidis and Meddah, 2024), the shape of the foundation (Pantelidis, 2025), and the depth of the foundation (Pantelidis, 2024).

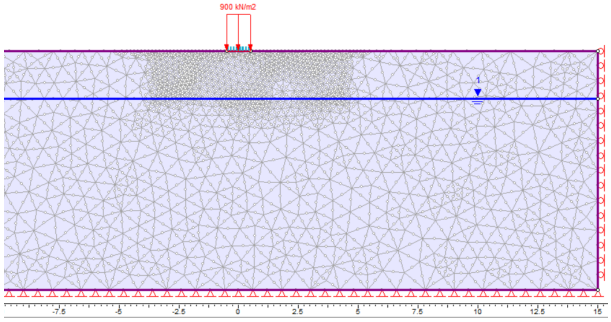

Figure 9. The finite element model used in the application example.

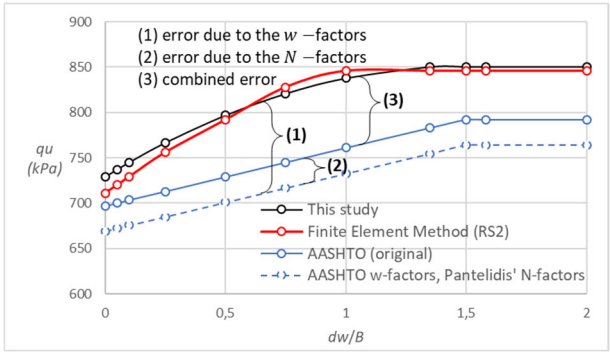

Figure 10. Application example: Comparison of the ultimate bearing capacity (q_u) derived by the AASHTO method, finite element analysis, and the proposed method for d_w/B ranging from 0 to 2.

6 CONCLUSIONS

This study proposed a fully analytical methodology for evaluating the effect of the groundwater table on the bearing capacity of shallow foundations. A key feature of the proposed approach is that the groundwater table correction factors were derived using the same classical earth pressure-based analysis method that was previously used for the derivation of the bearing capacity N-factors. This methodological consistency ensures coherence and reliability in the proposed bearing capacity formulation, in contrast to existing empirical methods that often introduce water table effects through separate and less rigorous adjustments. The comparison of the proposed method with several well-known approaches from the literature (e.g., Meyerhof, Vesic, Hansen, AASHTO, Bowles, Ausilio and Conte, Krishnamurthy and Rao) revealed significant differences, demonstrating the limitations and inconsistencies inherent in traditional empirical formulations. Importantly, the validity of the proposed analytical approach was verified against finite element method (FEM) results obtained through RS2 software. The agreement between the proposed method and the FEM results was excellent across a wide range of d_w/B ratios, from 0 to 2. This high level of agreement highlights the robustness of the proposed formulation and confirms its ability to accurately capture the effects of groundwater conditions on bearing capacity without resorting to empirical assumptions or fitting procedures. Additionally, the comparison with the AASHTO method showed that while the AASHTO predictions follow the same general trend, they tend to underestimate the bearing capacity for the case studied. This further underscores the advantage of the proposed method in providing a theoretically sound and accurate estimation. Overall, the fully analytical nature of the methodology, its internal consistency, and the strong agreement with numerical simulations offer a significant advancement in the assessment of bearing capacity under fluctuating groundwater conditions, enhancing both the theoretical understanding and practical application in geotechnical engineering design.

7 REFERENCES

AASHTO. 2020. LRFD Bridge Design Specifications (9th ed.). American Association of State Highway and Transportation Officials.

Bowles, J.E. 1996. Foundation analysis and design. McGraw-Hill, NY

De Simone, P., and Zurlo, R. 1987. The effect of groundwater table on the bearing capacity of shallow foundations. Proc. 9th European Conference on Soil Mechanics and Foundation Engineering (SMFE), Dublin, Vol. 2, 677–679.

Hansen, B., Denver, H., and Petersen, K. 1987. The influence of groundwater on bearing capacity of footings. Proc. 9th European Conference on Soil Mechanics and Foundation Engineering (SMFE), Dublin, Vol. 2, 685–690.

IS6403. 1981. Code of practice for determination of breaking capacity of shallow foundations. Bureau of Indian Standards.

Krishnamurthy, S., and Rao, N.K. 1975. Effect of submergence on bearing capacity. Soils and Foundations 15(3), 61–66.

Kimmerling, R. 2002. Geotechnical engineering circular No. 6 shallow foundations, FHWA-SA-02-054. United States. Federal Highway Administration. Office of Bridge Technology.

Meyerhof, G.G. 1955. Influence of roughness of base and ground-water conditions on the ultimate bearing capacity of foundations. Geotechnique 5(3), 227–242.

Pantelidis, L. 2023. Bearing capacity of centrically-vertically loaded strip foundations based on soil parameters: a classical earth pressure analysis problem. Preprint, Research Square, Version 2, 24 May 2023. Available at: https://doi.org/10.21203/rs.3.rs-2940474/v2

Pantelidis, L., Assefa, E., and Sachpazis, C. 2025. The effect of footing shape on the bearing capacity of shallow foundations: a review. Archives of Computational Methods in Engineering, 1–21.

Pantelidis, L., and Meddah, A. 2024. The effect of loading inclination and eccentricity on the bearing capacity of shallow foundations: a review. Archives of Computational Methods in Engineering 31(7), 4189–4208.

Pantelidis, L. 2024. Bearing capacity of shallow foundations: a focus on the depth factors in combination with the respective N-factors. Arabian Journal of Geosciences 17(6), 169.

Prandtl, L. 1920. Uber die harte plastischer korper. Nachr. Ges. Wissensch, Gottingen, Math.-Phys. Klasse, 1920, 74–85.

Terzaghi, K. 1925. Erdbaumechanik auf bodenphysikalischer Grundlage. Deuticke, Vienna.

Terzaghi, K. 1943. Theoretical Soil Mechanics. John Wiley & Sons. Available at: https://doi.org/10.1002/9780470172766

Vesic, A.S. 1973. Analysis of ultimate loads of shallow foundations. Journal of Soil Mechanics and Foundations Division, ASCE 99(1), 45–73.

Vesic, A.S. 1975. Bearing capacity of shallow foundations. In Foundation Engineering Handbook, edited by H.F. Winterkorn and H.Y. Fang, Van Nostrand Reinhold, New York, 121–147.